

Research Article

Experimental Study of Thermal Effect of Lacquer Coating for PV-Trombe Wall System Combined with Phase Change Material in Summer

Chenglong Luo ¹, Wu Zou,¹ Dan Sun,¹ Lijie Xu ², Jie Ji ² and Mengyin Liao¹

¹Institute of Energy Research, Jiangxi Academy of Sciences, Nanchang 330096, China

²Department of Thermal Science and Energy Engineering, University of Science and Technology of China, Hefei 230027, China

Correspondence should be addressed to Chenglong Luo; xxlong@ustc.edu

Received 4 April 2019; Revised 22 August 2019; Accepted 19 September 2019; Published 30 October 2019

Guest Editor: Alireza Rezaniakolaei

Copyright © 2019 Chenglong Luo et al. This is an open access article distributed under the Creative Commons Attribution License, which permits unrestricted use, distribution, and reproduction in any medium, provided the original work is properly cited.

This paper proposes a novel PV-Trombe wall system combined with phase-change material, which is named as PV-PCM-Trombe system. The work mainly experimentally studies the effectiveness and characteristics of using phase change materials to improve the overheating problem of PV-Trombe wall in summer. Through experiments, the photoelectric performance of the system using phase-change board surfaces with and without a matte black paint lacquer are compared; moreover, the influence on thermal environment of building is evaluated. The results indicate the PV-PCM-Trombe wall system shows an effective cooling effect on PV cell in both experiments and that the surface lacquer coating treatment of PCM plates affects little the photoelectric performance of the system and can reduce the working temperature of PV cell.

1. Introduction

Building-integrated photovoltaic/thermal technology (BIPV/T) is an important technology for using solar energy that generates solar energy photovoltaic power while improving the thermal environment of buildings to efficiently use solar energy. This can be considered as a significant contribution to the implementation of sustainable development of the energy.

Recently, focusing on BIPV/T technology, many numerical and experimental studies have been carried out from various perspectives. Yang and Jie [1] established a heat transfer model for photovoltaic-wall integrated (PV-WALL) structure and concluded that the heat gain of PV-WALL structures could be significantly reduced in summer. Jie et al. [2, 3] presented a novel Trombe wall with PV cells (PV-Trombe), which theoretically and experimentally studied the effect of the PV-Trombe system on indoor temperature and electrical efficiency and found that the aesthetic value was much more than that of normal Trombe wall. Hu et al. [4] compared and analyzed the annual thermal performance and electric performance of three types of BIPV system, and the result showed that a PV blind-integrated

Trombe wall system (BIPVBTW) is superior to the other two systems in the total electricity saving and CO₂ emissions reduction. Dupeyrat et al. [5] studied the electric performance and thermal performance of PV/T solar collectors with different laminates and the results indicated that PV/T solar collectors could provide advantages over separated solar thermal and PV technologies in configuration of limited available space for solar collector area. Herrando et al. [6] established a system performance evaluation model and mainly analyzed the effects of cover ratio of cells and coolant flow rate on system performance. Koyunbaba and Yilmaz [7] researched energy performance comparison of single glass, double glass, and a-Si semitransparent PV module integrated on the Trombe wall facade of a model test room. The change in electrical efficiency by surface temperature of the PV module had been interpreted and the electrical power rate of the PV module had been designated. Zogou and Stapountzis [8] studied the flow and heat transfer of a BIPV/air wall system for building application. In this work, the results from flow visualization and hot wire anemometry measurements performed on the basic structural module of a double-skin photovoltaic (PV/T) facade were discussed. Jiang et al. [9]

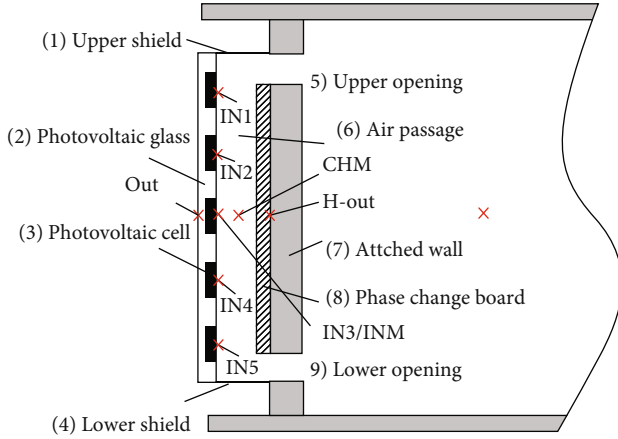


FIGURE 1: Schematic of structural principle of PV-PCM-Trombe wall system and the arrangement diagram of thermocouples.

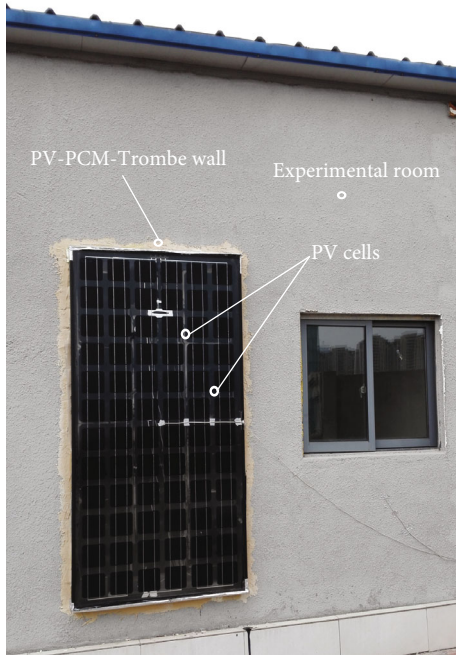


FIGURE 2: The test PV-PCM-Trombe wall system.

TABLE 1: Dimensions of the experimental setup.

Experimental setup	Length (m)	Height (m)	Width/thickness (m)
Hot box room	3.0	2.6	3.0
Door	0.6	1.6	—
Window	1.0	1.0	—
Upper/lower opening	0.3	0.2	—
Upper/lower shield	1.0	—	0.15
Photovoltaic glass board	1.0	2.0	0.004
Phase change board	0.3	0.5	0.02
Air passage	—	—	0.15
South wall	—	—	0.24

TABLE 2: Main properties of PCM.

Properties	Unit	Number
Melting point	$^{\circ}\text{C}$	29-31 (standard 29)
Solid point	$^{\circ}\text{C}$	26-28 (standard 26)
Latent heat (18-33 $^{\circ}\text{C}$)	kJ/kg	160
Solid density(20 $^{\circ}\text{C}$)	kg/L	1.43
Liquid density (40 $^{\circ}\text{C}$)	kg/L	1.23
Volume expansion rate	%	13.98
Thermal conductivity	W/(m·K)	0.6
Viscosity (50 $^{\circ}\text{C}$)	m^2/s	16.88

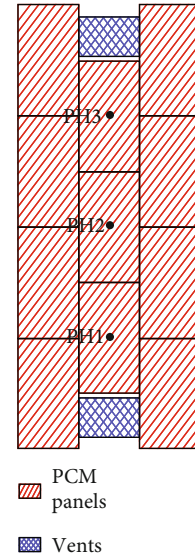


FIGURE 3: Distribution of phase change board and the thermocouples.

TABLE 3: Uncertainty of sensors at test conditions.

Copper-constantan thermocouples: temperature	$\pm 0.5^{\circ}\text{C}$
Pyranometer	Secondary standard (global irradiance on the south wall surface)
Output voltage: V_{oc}	1% of $V_{oc} \pm 0.1\text{ V}$
Output current: I_{sc}	1% of $I_{sc} \pm 9\text{ mA}$

presented a novel photovoltaic-Trombe wall (PV-TW). The electrical and thermal performance of the PV-TW are investigated experimentally and theoretically. Ahmed et al. [10] attempted to enhance the performance of a hybrid photovoltaic/Trombe wall (PV/TW) system through employing a porous medium. The results revealed that incorporating the porous medium and DC fan offered favorable features of the system performance, while the glass cover has a conflicting effect.

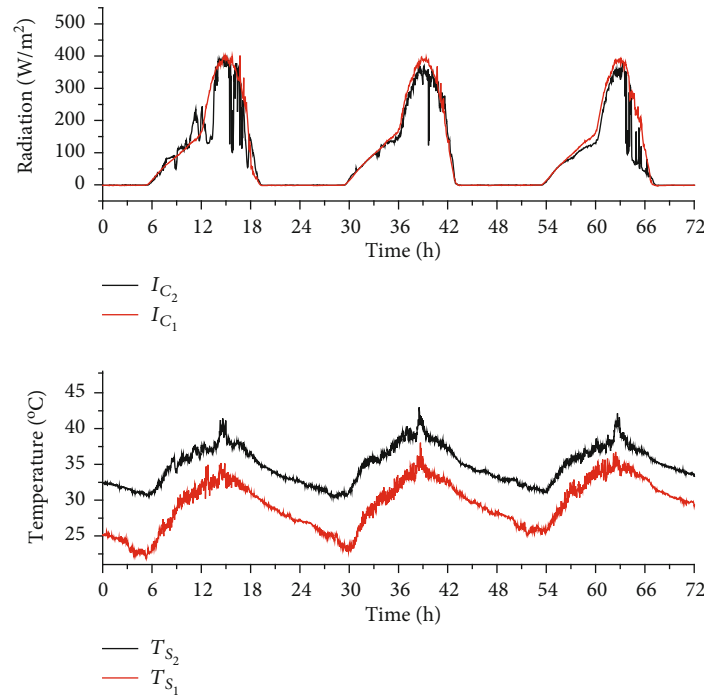


FIGURE 4: Solar irradiation intensity and ambient temperature.

Combining PCM (phase change material) and PV (photovoltaic) technologies to cool PV board or store heat by PCM has attracted scholars' attention. Huang [11–13] applied PCM to PV board and carried out many studies on the effect of PCM on the thermal regulation performance of BIPV systems. Lin et al. [14] floored all the internal walls of a room with PCM to study the influence of PV/T solar collector and PCM on indoor thermal environment. Through experiments and transient energy balance approach, Hachem et al. [15] and Kibria et al. [16] studied the effect of PCM on the performance of PV board and concluded that PCM could decrease the temperature of PV board and increase the electrical efficiency. Curpek and Hraska [17] compared and studied the PV board with and without PCM as well as the flow passage with and without ventilation, the results showed that natural ventilation of PV façade with added PCM could reduce the temperature of PV board better. Aelenei et al. [18, 19] developed a simplified thermal network model for BIPV-PCM and studied the thermal behavior of the system. Ma et al. [20] conducted a detailed review of the literature focusing on the use of PCM for PV module thermal regulation and electrical efficiency improvement and found that the PV-ST-PCM system, i.e., PV-PCM integrated with a solar thermal (ST) system, had an obvious scope for practical applications but met challenges.

Focusing on the inclination of solar heating wall of regular PV-Trombe wall system being overheated in summer working conditions, based on the feature that the temperature cannot rise during phase-change heating process of PCM, the present work proposes a novel PV-Trombe wall system combined with PCM, i.e., the PV-PCM-Trombe. The proposed system uses the thermal feature of PCM by combining the PCM and conventional PV-Trombe wall

TABLE 4: Test results of ambient temperature and solar irradiation intensity.

Date	Max. T_s (°C)	Mean T_s (°C)	Max. I_c (W/m ²)	Mean I_c (W/m ²)
2017.05.27	33.3	28.3	392.8	178.8
2017.05.28	34.8	29.3	388.5	181.2
2017.05.29	34.9	30.5	388.2	175.5
2017.07.14	39.7	34.5	379.5	155.2
2017.07.15	40.6	35.1	345.0	163.5
2017.07.16	40.3	35.0	364.5	126.6

system to reduce the temperature of solar heating wall in summer working conditions to avoid overheating issue of the wall resulted by solar radiation. This work mainly studies the effectiveness and characteristics of using phase change materials to improve the overheating problem of PV-Trombe wall in summer. Under summer working conditions, experimental investigations are carried out on a test system including the comparison of photoelectric performance of the novel system with and without matte black paint lacquer coating on phase-change board, and the analysis of their effects on thermal environment of the building.

2. Principle of PV-PCM-Trombe Wall System and the Experiment

The PV-PCM-Trombe wall system is composed of photovoltaic glass units, upper and lower openings, upper and lower shields, phase-change heat-storage wall, air passage, and a frame (Figure 1). The system is installed on the south

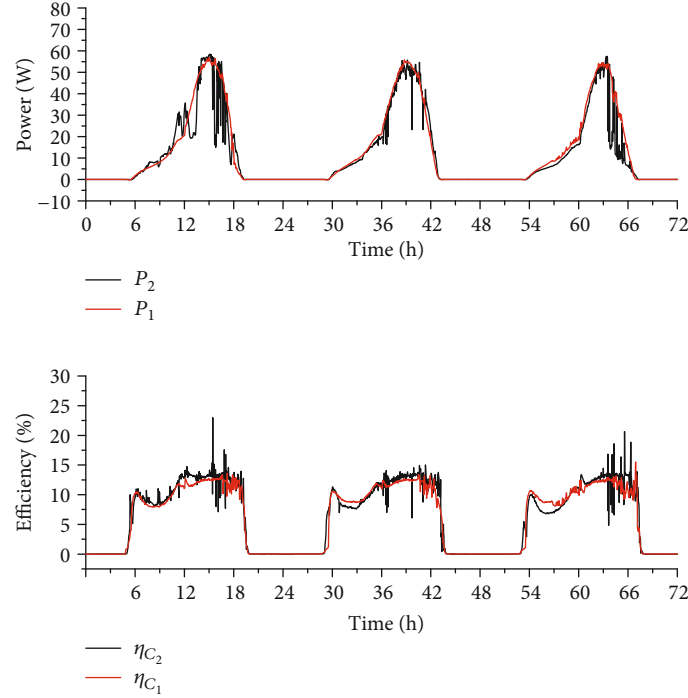


FIGURE 5: Electric power and efficiency of photovoltaic cells.

elevation (Figure 2), where the PCM board is attached to the external side of the south wall of building to form the PCM wall; the photovoltaic glass units cover the PCM wall and a certain gap is kept to form an air passage. By upper and lower openings and upper and lower shields, the system achieves passive heating in room in winter and heat dissipation to outdoor ambient to cool the room down in summer. Therefore, photoelectric conversion efficiency increases and indoor thermal environment improves. The design purpose of phase-change heat-storage wall is to use the characteristics of great phase-change energy storage, no increase in temperature during phase change process and phase-change temperature selected near the human comfort temperature; reduce the temperature of the passage where photovoltaic cells work especially in high-temperature summer while ensuring sufficient hot air supply in winter to meet the demand of building heating corresponding to human comfort temperature requirement; and achieve the overall effects of the system that the photovoltaic cells are cooled better and the photoelectric efficiency is higher, and the indoor thermal environment better meets the requirement of human comfort.

The working principle of the system is as follows.

1. Photovoltaic Part: the DC current generated by photovoltaic glass is converted into AC current
2. Solar Thermal Part

In summer, the upper opening (5) and the lower opening (9) are closed while the upper shield (1) and the lower shield (4) are opened so that the air passage (6) and the outdoor air forms a loop; thermal siphoning causes the air flowing

TABLE 5: Photovoltaic performance.

Date	Max. P (W)	Mean P (W)	Daily power generation (kW·h)	Mean η_c (%)
2017.05.27	55.4	23.5	0.322	10.7
2017.05.28	54.6	23.7	0.325	10.8
2017.05.29	54.1	22.3	0.299	10.5
2017.07.14	56.2	21.4	0.306	11.0
2017.07.15	51.8	22.2	0.318	10.6
2017.07.16	53.1	16.6	0.239	10.2

upwards from bottom in the passage, bringing away the heat absorbed by the phase-change heat-storage wall (7, 8) and the photovoltaic glass (2), and thereby the photovoltaic cells can be cooled down to some extent and overheating of the room in summer can be prevented. In addition, when the air temperature in the passage rises to the phase transition temperature of PCM, the PCM undertakes phase change process; the temperature can hardly rise as the PCM absorbs a significant amount of heat in the phase change process, and thus the rise of air temperature in the passage is inhibited and meanwhile, the photovoltaic cells and the building walls can be cooled down to some extent.

In winter, the upper opening (5) and the lower opening (9) are opened while the upper shield (1) and the lower shield (4) are closed so that the air passage (6) and the indoor room form a loop, bringing the heat absorbed by the phase change heat-storage wall (7, 8) and photovoltaic glass (2) into the room.

To investigate the system, a test system is established on a comparable hot box test platform. The experimental setup

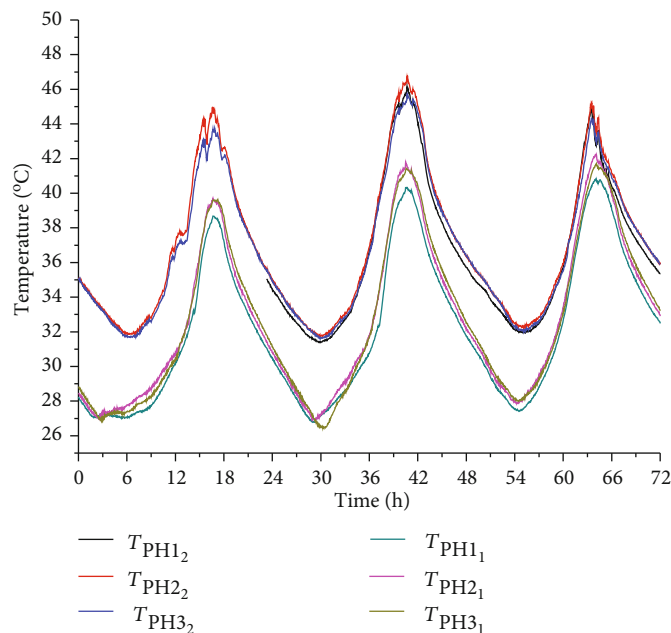


FIGURE 6: Temperature distribution of PCM plates.

TABLE 6: Characteristic data of mean temperature of external side temperature of phase change board 1, 2, and 3.

Temperature	Experiment 1			Experiment 2		
	Day 1	Day 2	Day 3	Day 1	Day 2	Day 3
Max. temperature (°C)	39.3	41.1	41.6	44.4	46.2	44.8
Mean temperature (°C)	31.3	32.6	33.5	36.4	37.1	36.6

consists of one hot box room, photovoltaic collector wall combined with PCM, openings, and a measurement system. Among them, the hot box room installed with photovoltaic collector wall combined with PCM is the experimental room. The south wall of both hot box rooms are brick structure, while other walls are lightweight insulating material. The dimensions of the experimental setup are shown in Table 1. The area of photovoltaic cells A_C is 1.125 m^2 , and the coverage ratio of photovoltaic cells on the photovoltaic glass board is 56.25%. The package material of PCM plate is aluminum, the surface is plated with a light color anticorrosion material, and the inner portion is crystalline hydrate and organic PCM; thus, the advantages of both PCMs, hydrate and organic matter, are met. The phase transition temperature of the PCM plates is 29°C ; its surface can be treated by matte black paint or kept as it is to perform comparable experimental analyses. The material properties of the PCM are listed in Table 2. The array configuration of the phase-change board is shown in Figure 3.

Measured parameters of the system include voltage, current, temperature, and solar irradiation intensity. Table 3 summarizes the ranges of parameters' accuracies. The temperature is measured using a conventional copper-constantan thermocouple (accuracy of $\pm 0.5^\circ\text{C}$). The main measuring points for temperature measurement are shown in Figures 1 and 3. Figure 1 represents a structural section

view of the system to show the locations of temperature measuring points marked by "x," i.e., external surface of photovoltaic glass board (1 point), back side of photovoltaic cells (5 points along height), air passage (1 point), external surface of the wall attached by phase change board (1 point), and indoor air temperature (1 point). Figure 3 presents the locations of the thermocouples distributed on the external surface of phase change heat storage board marked by "●." In addition, one thermocouple is placed on external surface of the south wall of experimental room. For the control room, there are two temperature measuring points which are indoor air temperature (1 point) and external surface of the south wall (1 point). The measurement system also includes the measurement of ambient temperature, output voltage and current of photovoltaic cells, and the total solar irradiation intensity on the south-faced vertical surface measured by a TBQ-2 pyranometer. DC voltage isolation sensor and AC-DC current isolation sensor are used, respectively, to detect the output voltage V_{oc} and current I_{sc} . The real-time acquisition of all data are done by an Agilent 34970A data acquisition instrument.

3. Experimental Results and Analysis

Experiments were carried out in Nanchang city in 2017, in three consecutive days on 27–29 May (experiment 1) and

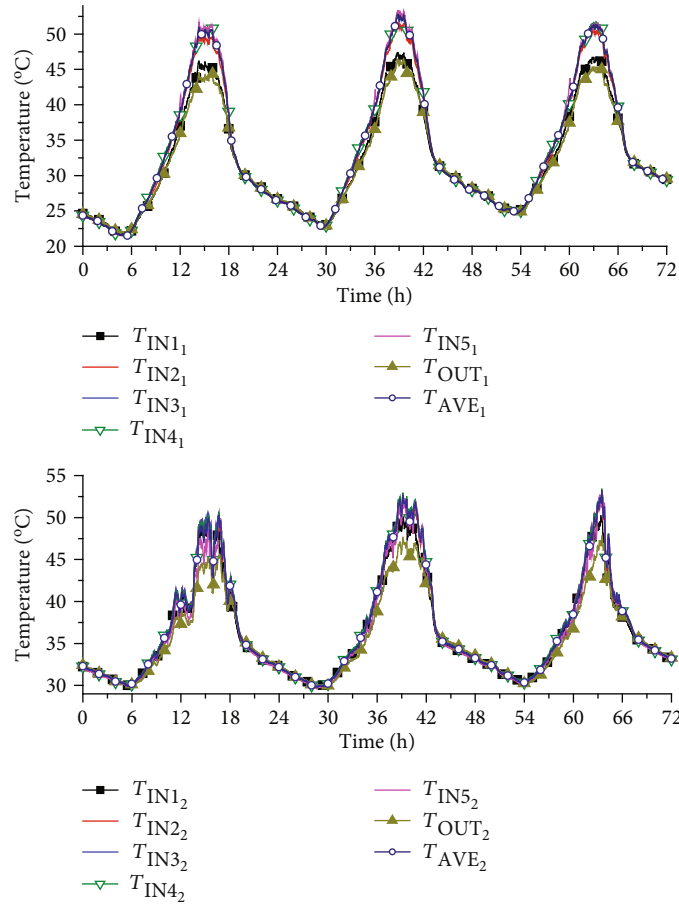


FIGURE 7: Inner and outer temperature distributions of PV cells.

TABLE 7: Test results of inner and outer temperatures of PV cells.

Date	T_{AVE} (°C)		T_{OUT} (°C)		Maximum difference between T_{AVE} and T_{OUT} (°C)
	Max. temperature	Mean temperature	Max. temperature	Mean temperature	
2017.05.27	50.5	32.1	44.0	30.6	6.5
2017.05.28	52.1	33.5	45.8	32.0	6.3
2017.05.29	51.1	34.2	45.1	32.7	6.0
2017.07.14	48.4	36.2	44.1	35.2	4.3
2017.07.15	51.4	37.3	46.7	36.1	4.7
2017.07.16	50.8	36.4	46.2	35.5	4.7

14-16 July (experiment 2). During the tests, the outdoor openings were kept open and the indoor openings closed, while room doors of the experimental room and the control room were kept open all the time. Matte black paint lacquer covered the external surface of the phase change board during the tests in July, like the treatment for the surface of the heating wall of a regular passive Trombe wall system. For the tests in May, the surface of the phase change board was not coated.

Figure 4 presents the distribution of solar irradiation intensity and ambient temperature during the three days of tests, and the detailed data is listed in Table 3 (mean ambient temperature is the average over a whole day; solar radiation is

the irradiation on the south-faced vertical wall, and its mean value is the average in the period from sunrise to sunset). I_c is the solar irradiation intensity and T_s is the ambient temperature. Their subscripts 1 and 2, respectively, represent experiment 1 and experiment 2. Based on Figure 4 and Table 4, the solar irradiation intensity of experiment 2 is slightly lower than that of experiment 1 on each corresponding day in the three days, while the ambient temperature is higher. The mean ambient temperature of experiment 1 is 29.4°C while that of experiment 2 is 34.9°C.

3.1. Power and Efficiency of Photovoltaic Cells. Electric power and photoelectric conversion efficiency are two important

parameters measuring the performance of photovoltaic cells. Through the definition of electric power $P = U \times I$, being U the voltage and I the current, electric power of photovoltaic cells can be calculated once voltage and current are measured. The photoelectric conversion efficiency can be obtained by Eq. (1).

Electric power of photovoltaic cells is given by

$$P = \eta_c I_c A_c, \quad (1)$$

where A_c is the area of photovoltaic cells, m^2 ; I_c is the solar irradiation intensity, W/m^2 ; and η_c is the photoelectric conversion efficiency.

Figure 5 presents the trends of electric power and efficiency of photovoltaic cells with time for experiments 1 and 2. P and η_c are the electric power and efficiency of photovoltaic cells, respectively. The electric powers and efficiencies of photovoltaic cells are similar between each pair of corresponding days in both experiments, and the efficiency varies in the range of 7%~13.5%. Table 5 lists the daily measured data from sunrise to sunset, i.e., at around 5:30~19:00 in experiment 1 and 5:15~19:30 in experiment 2. From the table, regarding experiment 1, the mean efficiency of power generation is about 10.7%, the daily mean power output is 23.1 W, and the daily power generation is 0.315 kW-h; for experiment 2, the mean efficiency of power generation is about 10.6%, the daily mean power output is 20.0 W, and the daily power generation is 0.287 kW-h. The difference in photovoltaic performance of photovoltaic cells is small between the two experiments, and the overall change characteristics are almost consistent. Thus, the matte black coating treatment slightly impacts on both electric power and efficiency of photovoltaic cells.

3.2. Temperature of PCM Plate. Figure 6 presents the external side temperatures of phase change boards 1, 2, and 3 (see Figure 3) in experiments 1 and 2. T_{PH} is the temperature of the external side of the PCM plate, and subscripts 1, 2, 3, respectively, represent PCM plates 1, 2, and 3. From the curves, all the external side temperatures of PCM plates 1, 2, and 3 in the two experiments are almost identical, and those in experiment 2 are higher than those in experiment 1. The external side temperatures of PCM plates 1, 2, and 3 are averaged, and the compared results of both experiments are listed in Table 5. According to Table 6, the highest temperature of the PCM plates in experiment 1 was 41.6°C and in experiment 2 46.2°C. On the one hand, the coating on the surface of the PCM plates in experiment 2 increases the absorption of solar heat. On the other hand, experiment 2 has a higher ambient temperature.

3.3. Cooling Effect on PV Cell. Figure 7 presents the temperatures at different height locations on the inner side and at the middle of the outer side of PV cells in experiments 1 and 2. T_{IN} is the temperature of each node along the high direction on the inner side of PV cells, and the subscript numbers 1-5 from small to large represents the high direction from low to high. T_{OUT} is the temperature at the middle of the outer side of PV cell. T_{AVE} is the mean temperature of the four locations

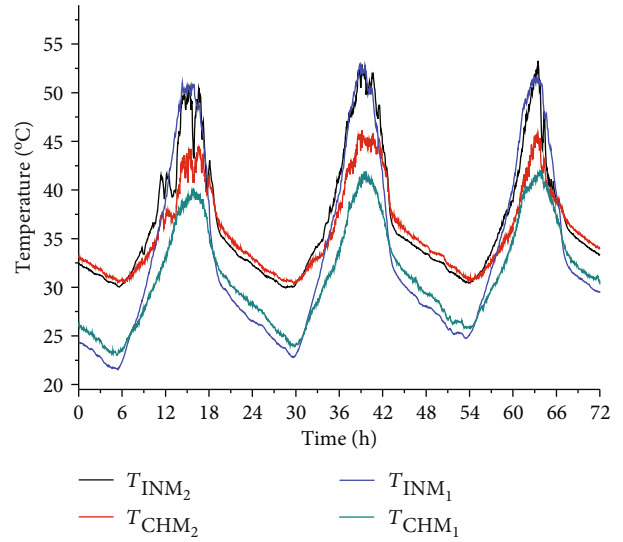


FIGURE 8: Inner side temperatures of PV cell and of the passage in the middle position.

in the upper part of the inner side of PV cell. As shown in the figure, during daytime, the internal temperatures are all higher than the outer temperature of PV cell; during nighttime, the internal temperatures at different height locations are close to the outer temperature of PV cell; the temperature distribution laws of PV cells are similar in both experiments. The specific data for T_{AVE} and T_{OUT} are listed in Table 7. As shown in the table, although the ambient temperature is higher in Experiment 2 and the maximum outer temperature of PV cells in experiment 2 is slightly higher than that of experiment 1, the internal maximum temperature of the PV cells in experiment 2 is slightly lower than that of experiment 1. The result shows that the absorption coating treatment on the surface of the PCM plates will increase the temperature of the PCM plates; however, there is a reduction in the working temperature of the PV cells.

Figure 8 shows the temperature in the middle of the inner side of PV cell and that of passage varying with time in experiments 1 and 2. T_{INM} is the temperature in the middle of the inner side of PV cell, and T_{CHM} is the temperature in the middle of passage. From the comparison between experiment 1 and experiment 2, the value of T_{INM} in experiment 2 is close to that in experiment 1, even slightly lower, but T_{CHM} in experiment 2 is higher than that in experiment 1. The results also indicate that the absorption coating treatment on the surface of the PCM plates can reduce the working temperature of PV cell. Table 8 lists the specific test results of the two experiments. The maximum value of T_{INM} is 52.3°C in experiment 1 and it is 51.7°C in experiment 2. The maximum values of T_{CHM} are 41.4°C and 45.3°C in experiments 1 and 2, respectively. The temperature difference between the inner side of PV cell and the passage reaches 11.6°C in experiment 1 and 6.7°C in experiment 2. According to [21], without a ventilation passage on the PV wall, the working temperature of PV cell reaches up to 70°C in summer. From the comparison,

TABLE 8: Test results of the inner side temperatures of PV cell and passage temperatures in the middle position.

Date	T_{INM} ($^{\circ}\text{C}$)		T_{CHM} ($^{\circ}\text{C}$)		Maximum difference between T_{INM} and T_{CHM} ($^{\circ}\text{C}$)
	Max. Temperature	Mean temperature	Max. Temperature	Mean temperature	
2017.05.27	50.6	32.2	39.6	30.2	11.6
2017.05.28	52.3	33.6	41.3	31.4	11.4
2017.05.29	51.4	34.3	41.4	32.3	10.3
2017.07.14	49.2	36.5	43.1	35.3	6.5
2017.07.15	51.7	37.5	45.3	36.2	6.5
2017.07.16	51.2	36.6	44.6	35.6	6.7

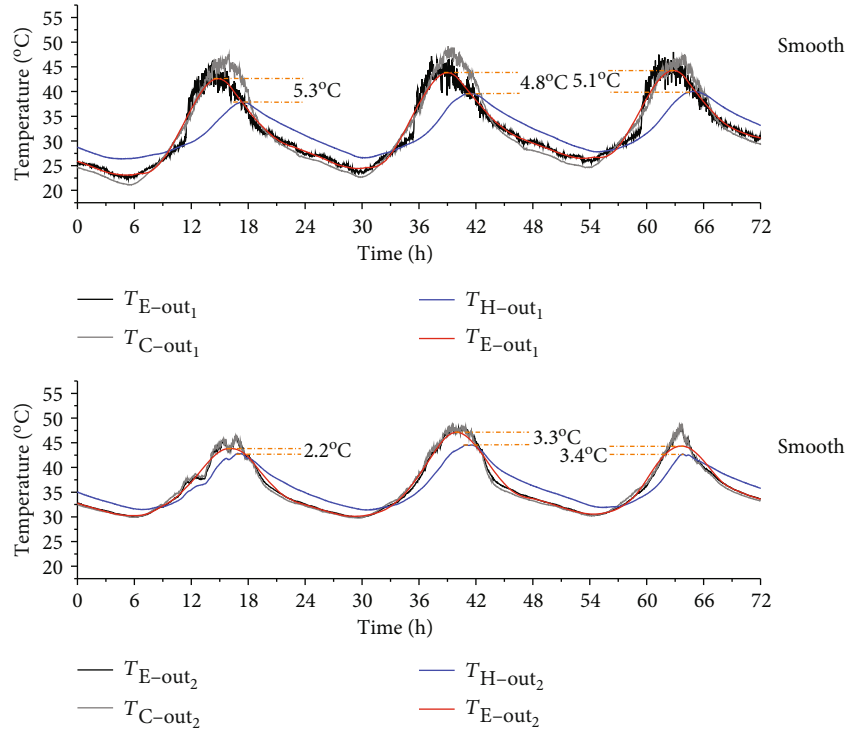


FIGURE 9: External side temperatures of the south wall and the Trombe wall.

the PV-PCM-Trombe wall system shows the effective cooling effect on PV cell both in experiments 1 and 2.

3.4. Thermal Effect on the Indoor Room. As is shown in Figure 9, $T_{\text{E-out}}$, $T_{\text{C-out}}$, and $T_{\text{H-out}}$ are, respectively, the temperatures of the external side of the south wall of experimental room, south wall of the control room, and Trombe wall in experiments 1 and 2. $T_{\text{E-out smooth}}$ is the smoothed curve of $T_{\text{E-out}}$. For each of experiments 1 and 2, the two temperature curves of the external side of the south wall of the experimental room and control room are almost coincident with each other; in daytime, the temperatures of the external side of the south wall of the experimental room and control room are higher than that of the Trombe wall which means that the passive solar building will not result in summer overheating problem of the wall, and the peak of temperature occurs earlier; in nighttime, the temperature of the external side of

the Trombe wall is higher than the that of others. From the comparison between the two experiments, the main characteristic is that the peak temperature difference between the south wall and the Trombe wall for the experimental room are lower in experiment 2. Take day 2 as an example, as is given by Table 9, the delay is 2 hours in experiment 1 and 40 minutes in experiment 2. In addition, the maximum value of $T_{\text{C-out}}$ in experiment 1 is almost the same as that of experiment 2, but the maximum values of $T_{\text{E-out}}$ and $T_{\text{H-out}}$ in experiment 2 are slightly greater than those in experiment 1; in each experiment, the daily mean values of $T_{\text{E-out}}$, $T_{\text{C-out}}$, and $T_{\text{H-out}}$ are substantially identical. Overall, though the coating on the external side of phase change board increases the solar heat absorption and the temperature of the Trombe wall slightly, the effect of preventing the wall from overheating in summer is still available for the passive solar system.

TABLE 9: Summarized results of the external side temperatures of the south wall and the Trombe wall.

Temperature and time	Experiment 1			Experiment 2		
	T_{E-out}	T_{C-out}	T_{H-out}	T_{E-out}	T_{C-out}	T_{H-out}
Max. temperature (°C)	44.4	47.7	39.6	47.8	47.8	44.5
Daily mean temperature (°C)	33.2	32.4	32.1	36.5	36.4	36.5
Day time to reach max.	14:11	15:17	17:21	16:19	16:17	17:01

4. Conclusions

Aiming at the summer overheating problem existing in regular PV-Trombe wall system, the present work proposes a novel PV-Trombe wall system combined with PCM, i.e., the PV-PCM-Trombe wall system. This work mainly experimentally studies the effectiveness and characteristics of using phase change materials to improve the overheating problem of PV-Trombe wall in summer. Through hot box experiments, two experiments were carried out in summer for comparing the proposed PV-Trombe wall system combined with phase change material (PV-PCM-Trombe system). Experiment 1 was carried out without coating the external surface of PCM plates, whereas in experiment 2, the external surface of the PCM plates was coated; in experiment 2, the solar irradiation intensity is slightly lower and the ambient temperature is higher. The following conclusions are addressed:

1. From the two experiments, electric power and the efficiency of photovoltaic cells are similar, so the coating treatment on the external surface of phase change board impacts a little on both electric power and efficiency of photovoltaic cells
2. The lacquer coating on the surface of the PCM plates can increase the absorption of solar heat. Therefore, it can increase the temperature of the PCM plates
3. The PV-PCM-Trombe wall system shows the effective cooling effect on PV cell compared with the regular PV-Trombe wall system, even the absorption coating treatment on the surface of the PCM plates can reduce the working temperature of PV cells
4. Though the coating on the external side of phase change board increases the solar heat absorption, the novel phase change heat storage-type PV-Trombe wall system will not induce room overheating whether the external surface of the phase change board is coated or not

The improvement of the PV-PCM-Trombe wall system is the use of phase change material layer. The above experimental results show that this improvement can help to avoid the summer overheating problem of the regular PV-Trombe wall system. In the future, this system will be further studied and optimized mainly from the aspects of theoretical modeling analysis and economic analysis.

Data Availability

All data used to support the findings of this study are included within the article.

Conflicts of Interest

The authors declare that they have no conflicts of interest.

Acknowledgments

This study was sponsored by the National Science Foundation of China (NSFC), (1) Project No. 51408278 and (2) No. 21663013.

References

- [1] H. Yang and J. Jie, "Study on the heat gain of a PV wall," *Acta Energiac Solaris Sinica*, vol. 20, no. 3, pp. 270–273, 1999.
- [2] J. Jie, Y. Hua, H. Wei, P. Gang, L. Jianping, and J. Bin, "Modeling of a novel Trombe wall with PV cells," *Building and Environment*, vol. 42, no. 3, pp. 1544–1552, 2007.
- [3] J. Ji, H. Yi, G. Pei, B. Jiang, and W. He, "Study of PV-Trombe wall assisted with DC fan," *Building & Environment*, vol. 42, no. 10, pp. 3529–3539, 2007.
- [4] Z. Hu, W. He, J. Ji et al., "Comparative study on the annual performance of three types of building integrated photovoltaic (BIPV) Trombe wall system," *Applied Energy*, vol. 194, pp. 81–93, 2017.
- [5] P. Dupeyrat, C. Ménézo, and S. Fortuin, "Study of the thermal and electrical performances of PVT solar hot water system," *Energy & Buildings*, vol. 68, pp. 751–755, 2014.
- [6] M. Herrando, C. N. Markides, and K. Hellgardt, "A UK-based assessment of hybrid PV and solar-thermal systems for domestic heating and power: system performance," *Applied Energy*, vol. 122, no. 122, pp. 288–309, 2014.
- [7] B. K. Koyunbaba and Z. Yilmaz, "The comparison of Trombe wall systems with single glass, double glass and PV panels," *Renewable Energy*, vol. 45, pp. 111–118, 2012.
- [8] O. Zogou and H. Stapountzis, "Flow and heat transfer inside a PVT collector for building application," *Applied Energy*, vol. 91, no. 1, pp. 103–115, 2012.
- [9] B. Jiang, J. Ji, and H. Yi, "The influence of PV coverage ratio on thermal and electrical performance of photovoltaic-Trombe wall," *Renewable Energy*, vol. 33, no. 11, pp. 2491–2498, 2008.
- [10] O. K. Ahmed, K. I. Hamada, and A. M. Salih, "Enhancement of the performance of photovoltaic/Trombe wall system using the porous medium: experimental and theoretical study," *Energy*, vol. 171, pp. 14–26, 2019.

- [11] M. J. Huang, "The effect of using two PCMs on the thermal regulation performance of BIPV systems," *Solar Energy Materials & Solar Cells*, vol. 95, no. 3, pp. 957–963, 2011.
- [12] M. J. Huang, P. C. Eames, and B. Norton, "Thermal regulation of building-integrated photovoltaics using phase change materials," *International Journal of Heat & Mass Transfer*, vol. 47, no. 12–13, pp. 2715–2733, 2004.
- [13] A. Hasan, S. J. McCormack, M. J. Huang, and B. Norton, "Evaluation of phase change materials for thermal regulation enhancement of building integrated photovoltaics," *Solar Energy*, vol. 84, no. 9, pp. 1601–1612, 2010.
- [14] W. Lin, Z. Ma, P. Cooper, M. I. Sohel, and L. Yang, "Thermal performance investigation and optimization of buildings with integrated phase change materials and solar photovoltaic thermal collectors," *Energy & Buildings*, vol. 116, pp. 562–573, 2016.
- [15] F. Hachem, B. Abdulhay, M. Ramadan, H. el Hage, M. G. el Rab, and M. Khaled, "Improving the performance of photovoltaic cells using pure and combined phase change materials - experiments and transient energy balance," *Renewable Energy*, vol. 107, pp. 567–575, 2017.
- [16] M. A. Kibria, R. Saidur, F. A. Al-Sulaiman, and M. M. A. Aziz, "Development of a thermal model for a hybrid photovoltaic module and phase change materials storage integrated in buildings," *Solar Energy*, vol. 124, pp. 114–123, 2016.
- [17] J. Curpek and J. Hraska, "Simulation study on thermal performance of a ventilated PV Façade coupled with PCM," *Applied Mechanics & Materials*, vol. 861, pp. 167–174, 2017.
- [18] L. Aelenei, R. Pereira, A. Ferreira, H. Gonçalves, and A. Joyce, "Building integrated photovoltaic system with integral thermal storage: a case study," *Energy Procedia*, vol. 58, pp. 172–178, 2014.
- [19] L. Aelenei, R. Pereira, H. Gonçalves, and A. Athienitis, "Thermal performance of a hybrid BIPV-PCM: modeling, design and experimental investigation," *Energy Procedia*, vol. 48, pp. 474–483, 2014.
- [20] T. Ma, H. Yang, Y. Zhang, L. Lu, and X. Wang, "Using phase change materials in photovoltaic systems for thermal regulation and electrical efficiency improvement: a review and outlook," *Renewable & Sustainable Energy Reviews*, vol. 43, pp. 1273–1284, 2015.
- [21] H. Hulin, H. Dong, and L. Kong, "Theoretical and experimental research on the natural convection cooling for solar cell," *Acta Energiac Solaris Sinica*, vol. 27, no. 3, pp. 309–313, 2006.



Hindawi

Submit your manuscripts at
www.hindawi.com

